Published in final edited form as:
Plast Reconstr Surg. 2014 July ; 134(1): 51–59. doi:10.1097/PRS.0000000000000287.

Sustained delivery of rhBMP-2 via PLGA microspheres: cranial bone regeneration without heterotopic ossification or craniosynostosis

Jason D. Wink, MD, MTR [Medical Student/ Basic Science Research Fellow],
Division of Plastic Surgery The Perelman School of Medicine at the University of Pennsylvania Children's Hospital of Philadelphia jwink3@gmail.com

Patrick A. Gerety, MD,
Division of Plastic Surgery The Perelman School of Medicine at the University of Pennsylvania Children's Hospital of Philadelphia Patrick.gerety@gmail.com

Rami D. Sherif,
Undergraduate Research Fellow Division of Plastic Surgery University of Pennsylvania College of Arts and Sciences Children's Hospital of Philadelphia rdsherif@gmail.com

Youngshin Lim, PhD,
Division of Plastic Surgery The Children's Hospital of Philadelphia limyoungshin@gmail.com

Nadya A.Clarke, MD,
Division of Plastic Surgery The Perelman School of Medicine at the University of Pennsylvania Children's Hospital of Philadelphia Nadya.clarke@nyumc.org

Chamith S. Rajapakse, PhD [Research Associate],
Department of Radiology The Perelman School of Medicine at the University of Pennsylvania chamith@mail.med.upenn.edu

Corresponding Author: Jesse A. Taylor, MD The Perelman School of Medicine at the University of Pennsylvania The Children's Hospital of Philadelphia Colket Translational Research Building 3501 Civic Center Blvd. 9th Floor Philadelphia, Pennsylvania 19104 Phone: (215) 590-2214 Fax: (215) 590-2496 Taylorj5@email.chop.edu.

Presentation History:
Data from this manuscript was accepted as a poster at the American Association of Plastic Surgeons Annual Meeting April 20-23, 2013 New Orleans, LA, and as podium presentations at the Plastic Surgery Research Council Annual Meeting May 2-4, 2013 in Santa Monica, CA, 12th International Congress on Cleft Lip/Palate and Related Craniofacial Anomalies May 5-10, 2013 in Orlando, Fl and the 15th Congress of the International Society for Craniofacial Surgery September 10-14, 2013 in Jackson Hole, WY.

Institutional Review Board:
This study was reviewed and approved by the Institutional Animal Care and Use Committee at the Children's Hospital of Philadelphia

Conflict of Interest:
No conflicts of interest to disclose

Financial Disclosures:
None of the authors has a financial interest in any of the products, devices, or drugs mentioned in this manuscript.

Authorship Participation and Contributions:
Jason D. Wink, MD, MTR: Data analysis, data interpretation, manuscript preparation Patrick A. Gerety, MD: Data analysis, data interpretation, manuscript preparation Rami Sherif: Data analysis, data interpretation, manuscript preparation Youngshin Lim, PhD: Data analysis, data interpretation, manuscript preparation Nadya Clarke, MD: Data analysis, data interpretation, manuscript preparation Chamith Rajapakse, PhD: Data analysis, data interpretation, manuscript preparation Hyun-Duck Nah, DMD PhD: Study conception, Data interpretation, manuscript preparation Jesse A. Taylor, MD: Study conception, data interpretation, manuscript preparation

Hyun-Duck Nah, DMD PhD [Research Associate Professor of Surgery], and
Division of Plastic Surgery The Perelman School of Medicine at the University of Pennsylvania The Children's Hospital of Philadelphia nah@email.chop.edu

Jesse A. Taylor, MD [Assistant Professor of Surgery]
Division of Plastic Surgery The Perelman School of Medicine at the University of Pennsylvania The Children's Hospital of Philadelphia Taylorj5@email.chop.edu

Abstract

Background—Commercially available recombinant human bone morphogenetic protein 2 (rhBMP2) has demonstrated efficacy in bone regeneration, but not without significant side effects. In this study, we utilize rhBMP2 encapsulated in PLGA microspheres (PLGA-rhBMP2) placed in a rabbit cranial defect model to test whether low-dose, sustained, delivery can effectively induce bone regeneration.

Methods—rhBMP2 was encapsulated in 15% poly (lactic-*co*-glycolic acid), using a double emulsion, solvent extraction/evaporation technique, and its release kinetics and bioactivity were tested. Two critical-size defects (10mm) were created in the calvarium of New Zealand White rabbits (5-7 mos of age, M/F) and filled with a collagen scaffold containing one of four groups: 1) no implant, 2) collagen scaffold only, 3) PLGA-rhBMP2(0.1ug/implant), or 4) free rhBMP2 (0.1ug/implant). After 6 weeks, the rabbits were sacrificed and defects were analyzed by μCT, histology, and finite element analysis.

Results—RhBMP2 delivered via bioactive PLGA microspheres resulted in higher volumes and surface area coverage of new bone than an equal dose of free rhBMP2 by μCT and histology ($p=0.025$, 0.025). FEA indicated that the mechanical competence using the regional elastic modulus did not differ with rhBMP2 exposure ($p=0.70$). PLGA-rhBMP2 did not demonstrate heterotopic ossification, craniosynostosis, or seroma formation.

Conclusions—Sustained delivery via PLGA microspheres can significantly reduce the rhBMP2 dose required for de novo bone formation. Optimization of the delivery system may be a key to reduce the risk for recently reported rhBMP2 related adverse effects.

Level of Evidence—Animal Study

Introduction

Recombinant human Bone Morphogenetic Protein 2 (rhBMP2) has been demonstrated to promote osteogenesis and is currently FDA approved for clinical use in spinal fusion, treatment of long bone fractures, sinus surgery and the repair of alveolar defects[1,2]. RhBMP2, as it is currently available (INFUSE, Medtronic Sofamor Danek, Memphis, TN), is delivered at approximately 1.5mg/cc[3] with patients receiving 2-14mg per treatment[4]. In these concentrations and doses, it has demonstrated efficacy in bone regeneration and bony union[5], but not without significant side effects[6] including heterotopic ossification (HO)[7-9], transient bone resorption[10], wound complications[11], local inflammation[12] and seroma formation[4, 13, 14]. Such side effects are poorly tolerated in anatomic regions requiring precise control over bone morphology and geometry, like the head and neck. This is especially important in the pediatric patient, with animal studies suggesting an interaction of

rhBMP2 and the growing brain[15] and the premature fusion of cranial sutures[16]. There have been numerous attempts to achieve the ideal delivery— timing, concentration, dose, vehicle-- of rhBMP2 for the repair of calvarial defects, but the ideal system remains elusive[9, 13, 14, 17].

In normal physiologic conditions, endogenous BMP2 is secreted by various cell types as an inactive precursor becoming tightly bound within the extracellular matrix. Under the conditions of bony injury and repair, it is released from the matrix and activated via enzymatic digestion to initiate receptor-mediated signaling in target cells. Studies have shown that demineralized bone has its own BMP2 carrier systems that are able to efficiently release BMP2 into the extracellular matrix at low doses and in a sustained manner during bone healing[18,11]. The purpose of this study is to measure the osteogenic efficacy of sustained release rhBMP2 utilizing a poly-lactic-co-glycolic acid (PLGA) microsphere delivery system loaded onto an FDA approved collagen sponge. Our primary endpoint is quantity of regenerated bone, with secondary endpoints being histologic analysis, biomechanical properties, and the presence of side effects.

Materials and Methods

PLGA-rhBMP2 Microspheres

rhBMP2 was encapsulated in 15% poly (lactic-*co*-glycolic acid) (PLGA) (66-107 kDa, 75:25) (Sigma- Aldrich; St. Louis, MO.), using a double emulsion solvent extraction/ evaporation technique[19]. Microspheres were lyophilized and stored at -80°C until use. Protein release kinetics were determined using the same PLGA microspheres encapsulating bovine serum albumin (BSA) (Sigma- Aldrich; St. Louis, MO.) Protein quantification was done by incubating microspheres at 37°C and measuring protein release using a bicinchoninic acid (BCA) assay kit (Thermo Scientific; Rockford, IL.). Encapsulation efficiency was determined by dissolving PLGA microspheres in dichloromethane (Sigma-Aldrich; St. Louis, MO) and performing a BCA assay to determine total quantity of protein encapsulated. This calculation ensured that the proper quantity of microspheres was added to achieve 0.1ug rhBMP2/implant. Bioactivity of PLGA-rhBMP2 was determined in co-culture with pre-osteoblastic MC3T3 cells based on alkaline phosphatase activity.

Preparation of Collagen Scaffolds

Immediately prior to implantation, native collagen scaffolds (Duragen®, Integra LifeSciences; Plainsboro, NJ) with a mean volume of 205.15+/-11.27um^3 were loaded with PLGA-rhBMP2 (0.1ug rhBMP2/implant) or free rhBMP2 (0.1ug/implant). To verify microsphere loading and distribution, rhodamine labeled microspheres were used and evaluated with fluorescent microscopy.

Surgery/Implantation

All procedures were conducted in accordance with guidelines from the institutional animal care and use committee. Anesthesia was initiated by intramuscular injection of ketamine/ xylazine (50mg/kg, 2.5mg/kg) and maintained on isoflurane (1-5% per L O_2). Prior to

incision, rabbits received a subcutaneous dose of buprenorphine (0.05mg/kg), intravenous dose of cefazolin (20mg/kg) and a fentanyl patch (25mcg/hr/72hrs).

Seven New Zealand White rabbits (Covance; Princeton, N.J.), 5-7 months of age, male and female, underwent bilateral, circular, 10mm craniectomy with a fine pineapple burr on a Midas Rex surgical drill (Medtronic Sofamor Danek; Memphis, TN) (Figure 1). Two implant placements were chosen randomly from 1 of 4 experimental groups (Table 1) in each animal. Care was taken to avoid injuring the underlying dura. Each implant was placed in the respective defect (Figure 1) and a single layer closure was performed. Post-op analgesia was delivered based on the veterinary staff's assessment of the animal's discomfort.

After 42+/-2 days, rabbits underwent euthanasia with initial intramuscular injection of ketamine/xylazine (50mg/kg, 2.5mg/kg), lethal intravenous overdose of pentobarbital (125 mg/kg) and thoracotomy. Following dissection, samples were fixed in 37% formalin (Sigma-Aldrich; St. Louis, MO.) for 1-2 weeks prior to decalcification.

MicroCT

Bone regeneration was assessed using micro-computed tomography (μCT) with 30um slice thickness (VivaCT40; Scanco Medical, Easton, PA.). μCT was performed after sample harvest and formalin fixation, prior to decalcification. 3-D reconstruction using standard bone thresholding and quantitative analysis of new bone was performed, measuring volume and surface area of new bone using commercially available software (Mimics, Materialise; Leuven, Belgium). Each sample was analyzed in a qualitative manner by two independent observers for the presence of HO and craniosynostosis.

Finite Element Analysis (FEA)

Post-hoc FEA was performed on all samples to understand the mechanical properties of newly formed bone using Rajapakse's technique[20-23]. μCT data was resliced to ensure that mechanical modeling was performed with simulated loading in the cranial-caudal axis (C-C). Three, 1530um x 1530um x 330um regions of interest (ROI) were chosen (third dimension along the C-C axis) for each rabbit sample to include an area on the medial edge of each defect site, a control sample of unaltered calvarium on the midline adjacent to the two defect sites and a region on the medial portion of the defect margin.

FEA was performed on each ROI by modeling a compressive force in the cranial-caudal axis. A micro-scale bone tissue modulus of 20GPa for native calvarium, a conservative estimate of 18GPa for regenerated calvarium and 0.3 Poison's ratio[24] was chosen for the analysis based on previous nano-indentation results in a rabbit cranial model[25]. In the defect margin ROI, native and regenerated bone were outlined and the respective micro-scale tissue modulus was applied. The lateral surfaces of the ROI were constrained to mimic *in situ* bone conditions. Regional Young's modulus / apparent stiffness and stress maps were generated by solving the finite-element system[21]. Analyses were performed by grouping ROIs into native calvarium vs. defect site, exposure to PLGA-rhBMP2 vs. exposure to free rhBMP2, and defect margin vs. bone regenerate and native calvarium.

Histology

Following radiographic analysis, samples were decalcified in formic acid (ImmunoCal™; decal® Tallman, N.Y.) for 14 days before undergoing processing and paraffin embedding. Five μm thick sections were taken across the central region of each defect and stained with H&E and trichrome. Defect margins were clearly visible based on differences in bone trabecular morphology.

Statistical Analysis

Kruskal- Wallis multiple comparison testing was performed when comparing greater than two groups. Individual subgroup analyses of bone volume, surface area and regional Young's were performed using Mann-Whitney tests, with the most important comparison being 0.1ug PLGA-rhBMP2 vs. 0.1ug Free rhBMP2. All statistical tests on bone quantity were performed in a one-sided manner with significance determined by $p<0.05$ due to our initial hypothesis that the introduction of growth factor would improve bone growth. Statistical testing on bone quality (FEA) was performed in a two-sided manner with significance determined by $p<0.05$.

Results

Scaffold Loading and In Vitro Assays

Microspheres were generated ranging in diameter from 5.55um to 125.18um , with a mean of 54.85+/-27.61um. Based on the release kinetics of BSA encapsulated in our PLGA microspheres *in vitro*, rhBMP2 is released in a logarithmic fashion with 30% of encapsulated rhBMP2 released in a burst fashion within the first 24 hours and the remainder delivered in a sustained manner over 35 days (Figure 2). Bioactivity of PLGA-rhBMP2 was confirmed by its ability to induce alkaline phosphatase activity in a co-culture with a pre-osteoblastic cell line (MC3T3) (Figure 2). Empty PLGA microspheres had no effect on alkaline phosphatase induction. Visual inspection, as well as fluorescence microscopy, revealed a heterogenous microsphere sample that was loaded efficiently on our scaffold prior to implantation (Figure 3).

Computed Tomographic Image Analysis

New bone volume and surface area were compared among different experimental groups by μCT. Kruskal Wallis multiple comparisons test was first performed on bone volume ($p=0.031$) and surface area ($p=0.032$). Volume analysis showed that the PLGA-rhBMP2 group (0.1ug rhBMP2/implant) (49.25+/-9.13mm^3) outperformed both the empty control (20.21+/-8.78mm^3, $p=0.025$) and 0.1ug rhBMP2 group (37.51+/-2.25mm^3, $p=0.025$) (Figure 4). Surface area analysis showed that the PLGA-rhBMP2 group covered 63.59 mm2 +/-6.95mm^2 of the defect site, outperforming the untreated control (42.54+/-14.42 mm^2 ($p=0.025$)), scaffold only control (45.06+/-10.07mm^2 ($p=0.010$)), and equivalent dose of free rhBMP2 (52.06+/-4.16mm^2 ($p=0.025$)) (Figure 4, Table 2). None of the experimental samples exhibited heterotopic ossification, craniosynostosis, or seroma formation (Table 2)

Histologic Analysis

The qualitative analysis of histologic sections of all samples with H&E and trichrome staining revealed varying stages of calcified bone regenerate in each experimental group. Representative sections appeared to form bone through endochondral ossification with multiple samples showing a cartilage intermediate (Figure 6). All new bone formed in a woven fashion with disorganized trabeculae, presence of neovascularization and osteoblasts around the periphery (Figure 6). The transition to a more mature lamellar phenotype was also present in some areas of new bone. The development of cortical tables and a new diploic space was not present in any defect sites. Negative and positive controls had defects that were filled with a collagenous scar and a small amount of bone regenerate around the edge of the defect.

A number of histological sections from microsphere containing groups had small quantities of adjacent microspheres. In many instances the microspheres were either infiltrated by, or adjacent to, multinucleated giant cells (Figure 6).

Finite Element Analysis

FEA was performed in order to investigate the relative mechanical competence of native calvarium and bone regenerate. Native calvarium was found to have a mean regional Young's modulus of 10.66 +/- 3.07GPa while bone regenerate regardless of experimental group had a mean regional Young's modulus of 8.31 +/- 2.15 GPa ($p=0.07$). There was no statistical difference between bone regenerate with and without rhBMP2 exposure ($p=0.70$) and based on the method of rhBMP2 delivery ($p=0.83$). (Table 3)

There was a significant difference between the trabeculation patterning of native versus regenerated bone. Regenerated bone appeared to have a much greater number of fine trabeculations when compared to the native calvarium (Figure 5). There did not appear to be a difference in patterning between rhBMP2-exposed bone regenerate and bone formed through the animal's intrinsic healing mechanisms. Further modeling of the stress found in the trabecular microenvironment appeared to indicate that stress is not evenly distributed to all trabeculae in both native and regenerated calvarium (Figure 5). At the defect margin it appears that native calvarium is the main load carrier and thus the physical properties of the margin are determined by the mechanical competence of the native calvarium (Figure 5, Table 3).

Discussion

At commercially available doses, rhBMP2 effectively enhances osteogenesis and bony union[5], but not without significant side effects[6] including heterotopic ossification[7-9], transient bone resorption[10], wound complications[11], local inflammation[12] , craniosynostosis[16], and seroma formation[4, 13, 14]. These side effects are believed to be secondary to high growth factor concentrations[3, 26] and may be poorly tolerated in anatomically sensitive areas such as the spine and craniofacial skeleton. In this study, we utilize a total dose of rhBMP2, which in our microspheres is spread out over approximately one month; this dose is approximately 10,000-100,000x less than the total dose that is

clinically utilized[4], the result being a significantly decreased local growth factor concentration. The dose in this study is also significantly lower than previously published work in this area[9, 13, 27-29]. Thus, we are beginning to ask and attempt to answer the question, what is the minimal dose and local concentration of rhBMP2 that can be delivered over time in order to induce bone regeneration without the production of unwanted side effects?

Both the free and encapsulated rhBMP2 group generated bone, and we demonstrate that 0.1ug PLGA-rhBMP2 group produced an increased volume and surface area of bone compared to an equal 0.1ug dose of free rhBMP2. Although our dosing strategy may not have been sufficient to achieve full defect closure at 42 days, it serves as a baseline from which future studies can be performed to optimize osteogenesis while minimizing side effects.

Bone formed with exposure to rhBMP2 demonstrated a similar histologic morphometry and mechanical competence to bone formed through native healing mechanisms. New bone appeared to form through endochondral ossification. Previous studies examining critically-sized defects of the calvarium[9, 13, 30, 31] were unable to find the presence of a cartilage intermediate in their newly formed bone. Bone growth induced by the delivery of rhBMP2 has been found to promote osteogenesis in both an endochondral and membranous fashion, varying based on the mode of rhBMP2 delivery[32, 33]. It is difficult to explain this difference, though one might postulate that we created a microenvironment in our implants that led to differing mechanisms of osteogenesis. This, in and of itself, is an interesting finding that deserves further investigation. It is also possible that the rate of cartilage to bone conversion may vary based on the dose of rhBMP2 used. At the low rhBMP2 dose utilized in our study, it is possible that we induced a slow rate of conversion and thus were able to visualize the preosteoid state.

A justified criticism of previous work in this area is the lack of testing of mechanical properties of engineered bone. To our knowledge this is the first study to use FEA to better understand the mechanical properties of both native calvarium and regenerated bone. Using this modeling technique, we were not able to show a statistically significant difference in the mechanical competence of regenerated bone compared to native calvarium, although post-hoc power calculations revealed that our study was under-powered to elucidate a difference. That said, it did appear that the inclusion of rhBMP2 did not affect the mechanical competence of bone regenerate. Adequate mechanical competency of the bone regenerate adds further validity to the clinical use of rhBMP2.

There are several limitations to this study using the methods outlined. The relative dispersion of our data remained high most likely due to the many layers of uncontrollable intrinsic variability in our experiment. Each rabbit may have differing intrinsic regeneration capacity, which we have not accounted for by including two experiments in each animal. There may have been minor variability in size and shape of the defects, though the random assignment of groups intra-operatively should have controlled for this, somewhat. Release kinetics were determined *in vitro* and growth factor release may potentially be accelerated or decelerated, *in vivo*. Closure was performed in one layer providing the potential for

interaction between each experimental sample. We feel that it is unlikely that a significant paracrine effect would occur as each sample was maintained inside of the delivery scaffold. Our experiment only allowed for analysis at a single time point, giving no indications of bone regeneration rates during the experimental period, or after further bone maturation. Increasing the experimental time may have also allowed our experimental groups to further outperform our controls. FEA has been validated for use in understanding the mechanical properties of long bones; however, we believe this is its first use to understand the properties of the calvarium. We have not performed testing to validate the mechanical analyses that were performed.

At all doses and delivery methods of rhBMP2 complete closure of the cranial defects was not achieved after 6 weeks, potentially due to insufficient doses in this animal model. Heterotopic ossification was not appreciated in this time period and it is unknown whether it would have occurred if the animals were followed for a longer duration. Our low dose was chosen based on previous *in vitro* work on the potency of free rhBMP2 at 20-50ng/ml[34, 35]. It is known that the necessary rhBMP2 dose varies between animal species[26]. The delivery method may also have led to uneven delivery of growth factor over the defect leading to asymmetric bone growth in some animals. Further studies will focus on these limitations with the hopes of translating to humans.

Conclusions

Sustained, low-dose rhBMP2 delivery via PLGA microspheres (0.1ug rhBMP2/implant) provides for enhanced osteogenesis when compared to an equal dose of free rhBMP2 (0.1ug rhBMP2/implant). Future work will continue to focus on the optimal dosing and scaffold delivery of encapsulated rhBMP2 to completely heal cranial defects in a safe and effective manner.

Acknowledgments

The authors are indebted to Dr. Jennifer McGrath and Imad Salhab for their work on the technical aspects of this study, Dr. Kudakwashe Chikwava (Children's Hospital of Philadelphia, Department of Pathology) for his assistance in interpreting our histologic specimens, the Children's Hospital of Philadelphia Pathology Core for their assistance in preparing our histologic specimens and Andrew J. Cucchiara, PhD (University of Pennsylvania Adjunct Professor of Biostatistics) for his assistance with the statistical analysis of our study.

Financial Support:

The project described was supported by the Department of Surgery at the Perelman School of Medicine at the University of Pennsylvania (JT), University of Pennsylvania Center for Human Appearance (PG, JT, HDN), American Association of Plastic Surgeons Academic Scholarship (JT), Department of Defense (HDN) and National Center for Research Resources and the National Center for Advancing Translational Sciences at the National Institutes of Health (JW)

References

1. McKay B. Local sustained delivery of recombinant human bone morphogenetic protein-2 (rhBMP-2). Conf Proc IEEE Eng Med Biol Soc. 2009; 2009:236–237. [PubMed: 19963455]
2. BMP 2--Genetics Institute/ Medtronic-Sofamor Danek/Integra. Bone morphogenetic protein 2--Genetics Institute/ Medtronic-Sofamor Danek/Integra, INFUSE Bone Graft, recombinant human bone morphogenetic protein 2--Genetics Institute/Medtronic-Sofamor Danek/Integra, RhBMP 2--

Genetics Institute/Medtronic-Sofamor Danek/Integra. BioDrugs. 2002; 16:376–377. [PubMed: 12408742]

3. McKay WF, Peckham SM, Badura JM. A comprehensive clinical review of recombinant human bone morphogenetic protein-2 (INFUSE Bone Graft). Int Orthop. 2007; 31:729–734. [PubMed: 17639384]
4. Garrett MP, Kakarla UK, Porter RW, Sonntag VK. Formation of painful seroma and edema after the use of recombinant human bone morphogenetic protein-2 in posterolateral lumbar spine fusions. Neurosurgery. 2010; 66:1044–1049. discussion 1049. [PubMed: 20495420]
5. Jones AL, Bucholz RW, Bosse MJ, et al. Recombinant human BMP-2 and allograft compared with autogenous bone graft for reconstruction of diaphyseal tibial fractures with cortical defects. A randomized, controlled trial. J Bone Joint Surg Am. 2006; 88:1431–1441. [PubMed: 16818967]
6. Woo EJ. Adverse Events After Recombinant Human BMP2 in Nonspinal Orthopaedic Procedures. Clin Orthop Relat Res. 2012
7. Shah RK, Moncayo VM, Smitson RD, Pierre-Jerome C, Terk MR. Recombinant human bone morphogenetic protein 2-induced heterotopic ossification of the retroperitoneum, psoas muscle, pelvis and abdominal wall following lumbar spinal fusion. Skeletal Radiol. 2010; 39:501–504. [PubMed: 20162273]
8. Anderson CL, Whitaker MC. Heterotopic ossification associated with recombinant human bone morphogenetic protein-2 (infuse) in posterolateral lumbar spine fusion: a case report. Spine (Phila Pa 1976). 2012; 37:E502–506. [PubMed: 22020605]
9. Kinsella CR Jr. Bykowski MR, Lin AY, et al. BMP-2-mediated regeneration of large-scale cranial defects in the canine: an examination of different carriers. Plast Reconstr Surg. 2011; 127:1865–1873. [PubMed: 21532416]
10. Kaneko H, Arakawa T, Mano H, et al. Direct stimulation of osteoclastic bone resorption by bone morphogenetic protein (BMP)-2 and expression of BMP receptors in mature osteoclasts. Bone. 2000; 27:479–486. [PubMed: 11033442]
11. Woo EJ. Adverse events reported after the use of recombinant human bone morphogenetic protein 2. J Oral Maxillofac Surg. 2012; 70:765–767. [PubMed: 22177811]
12. Perri B, Cooper M, Lauryssen C, Anand N. Adverse swelling associated with use of rh-BMP-2 in anterior cervical discectomy and fusion: a case study. Spine J. 2007; 7:235–239. [PubMed: 17321975]
13. Por YC, Barcelo CR, Salyer KE, et al. Bone generation in the reconstruction of a critical size calvarial defect in an experimental model. J Craniofac Surg. 2008; 19:383–392. [PubMed: 18362715]
14. Smith DM, Afifi AM, Cooper GM, Mooney MP, Marra KG, Losee JE. BMP-2-based repair of large-scale calvarial defects in an experimental model: regenerative surgery in cranioplasty. J Craniofac Surg. 2008; 19:1315–1322. [PubMed: 18812857]
15. Furuta Y, Piston DW, Hogan BL. Bone morphogenetic proteins (BMPs) as regulators of dorsal forebrain development. Development. 1997; 124:2203–2212. [PubMed: 9187146]
16. Kinsella CR Jr. Cray JJ, Durham EL, et al. Recombinant human bone morphogenetic protein-2-induced craniosynostosis and growth restriction in the immature skeleton. Plast Reconstr Surg. 2011; 127:1173–1181. [PubMed: 21364420]
17. Elsalanty ME, Por YC, Genecov DG, et al. Recombinant human BMP-2 enhances the effects of materials used for reconstruction of large cranial defects. J Oral Maxillofac Surg. 2008; 66:277–285. [PubMed: 18201609]
18. Peel SA, Hu ZM, Clokie CM. In search of the ideal bone morphogenetic protein delivery system: in vitro studies on demineralized bone matrix, purified, and recombinant bone morphogenetic protein. J Craniofac Surg. 2003; 14:284–291. [PubMed: 12826798]
19. Borselli C, Ungaro F, Oliviero O, et al. Bioactivation of collagen matrices through sustained VEGF release from PLGA microspheres. J Biomed Mater Res A. 2010; 92:94–102. [PubMed: 19165799]
20. Rajapakse CS, Leonard MB, Bhagat YA, Sun W, Magland JF, Wehrli FW. Micro-MR imaging-based computational biomechanics demonstrates reduction in cortical and trabecular bone strength after renal transplantation. Radiology. 2012; 262:912–920. [PubMed: 22357891]

21. Rajapakse CS, Magland JF, Wald MJ, et al. Computational biomechanics of the distal tibia from high-resolution MR and micro-CT images. Bone. 2010; 47:556–563. [PubMed: 20685323]
22. Wehrli FW, Rajapakse CS, Magland JF, Snyder PJ. Mechanical implications of estrogen supplementation in early postmenopausal women. J Bone Miner Res. 2010; 25:1406–1414. [PubMed: 20200948]
23. Zhang XH, Liu XS, Vasilic B, et al. In vivo microMRI-based finite element and morphological analyses of tibial trabecular bone in eugonadal and hypogonadal men before and after testosterone treatment. J Bone Miner Res. 2008; 23:1426–1434. [PubMed: 18410234]
24. Zysset PK, Guo XE, Hoffler CE, Moore KE, Goldstein SA. Elastic modulus and hardness of cortical and trabecular bone lamellae measured by nanoindentation in the human femur. Journal of Biomechanics. 1999; 32:1005–1012. [PubMed: 10476838]
25. Vayron R, Barthel E, Mathieu V, Soffer E, Anagnostou F, Haiat G. Nanoindentation measurements of biomechanical properties in mature and newly formed bone tissue surrounding an implant. J Biomech Eng. 2012; 134:021007. [PubMed: 22482674]
26. Zara JN, Siu RK, Zhang X, et al. High doses of bone morphogenetic protein 2 induce structurally abnormal bone and inflammation in vivo. Tissue Eng Part A. 2011; 17:1389–1399. [PubMed: 21247344]
27. DeCesare GE, Cooper GM, Smith DM, et al. Novel animal model of calvarial defect in an infected unfavorable wound: reconstruction with rhBMP-2. Plast Reconstr Surg. 2011; 127:588–594. [PubMed: 21285763]
28. Kinsella CR Jr. Cray JJ, Smith DM, et al. Novel model of calvarial defect in an infected unfavorable wound: reconstruction with rhBMP-2. Part II. J Craniofac Surg. 2012; 23:410–414. [PubMed: 22421834]
29. Kinsella CR Jr. Macisaac ZM, Cray JJ, et al. Novel Animal Model of Calvarial Defect: Part III. Reconstruction of an Irradiated Wound with rhBMP-2. Plast Reconstr Surg. 2012; 130:643e–650e.
30. Rapp SJ, Jones DC, Gerety P, Taylor JA. Repairing critical-sized rat calvarial defects with progenitor cell-seeded acellular periosteum: A novel biomimetic scaffold. Surgery. 2012; 152:595–605. e591. [PubMed: 22959744]
31. Wikesjo UM, Qahash M, Polimeni G, et al. Alveolar ridge augmentation using implants coated with recombinant human bone morphogenetic protein-2: histologic observations. J Clin Periodontol. 2008; 35:1001–1010. [PubMed: 18976397]
32. Kawai M, Bessho K, Maruyama H, Miyazaki J, Yamamoto T. Human BMP-2 gene transfer using transcutaneous in vivo electroporation induced both intramembranous and endochondral ossification. Anat Rec A Discov Mol Cell Evol Biol. 2005; 287:1264–1271. [PubMed: 16247797]
33. Kuboki Y, Saito T, Murata M, et al. Two distinctive BMP-carriers induce zonal chondrogenesis and membranous ossification, respectively; geometrical factors of matrices for cell-differentiation. Connect Tissue Res. 1995; 32:219–226. [PubMed: 7554920]
34. Wang L, Huang Y, Pan K, Jiang X, Liu C. Osteogenic responses to different concentrations/ratios of BMP-2 and bFGF in bone formation. Ann Biomed Eng. 2010; 38:77–87. [PubMed: 19921434]
35. Akino K, Mineta T, Fukui M, Fujii T, Akita S. Bone morphogenetic protein-2 regulates proliferation of human mesenchymal stem cells. Wound Repair Regen. 2003; 11:354–360. [PubMed: 12950639]

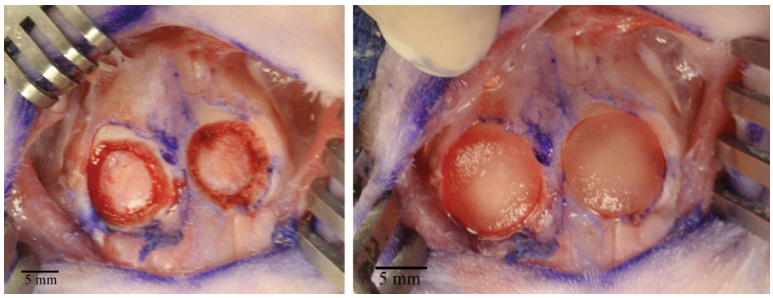

Figure 1.
Intraoperative view of 10mm bilateral defect creation (left) and placement of growth factor loaded scaffold into defect site (right)

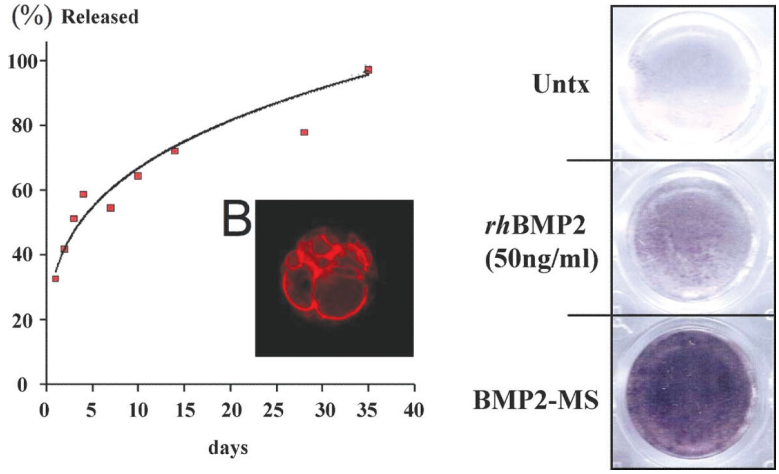

Figure 2.

Curve displaying release kinetics of BSA encapsulated in PLGA microspheres over 35 days (left). Color change representing alkaline phosphatase activity after co-culture of PLGA-rhBMP2 and pre-osteoblastic MC3T3 cells (right).

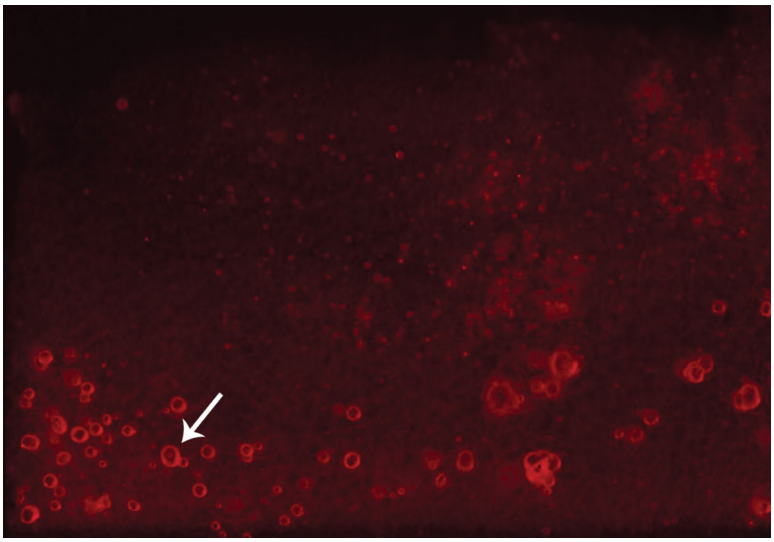

Figure 3.
Duragen scaffold under fluorescence microscopy. PLGA microspheres (arrow) loaded with rhodamine dye (red).

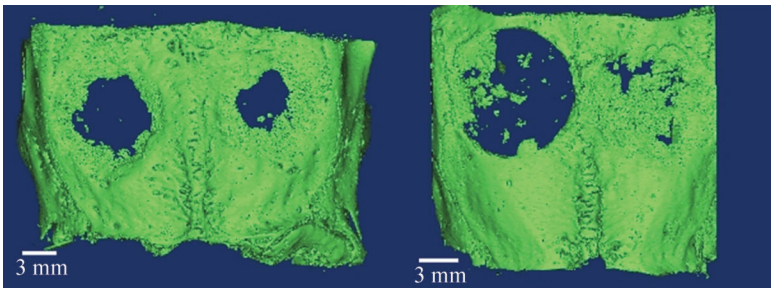

Figure 4.

Representative three-dimensional reconstructions of microCT data thresholded for bone. Each sample has two defects (L,R). Groups A, B (top left), Groups B, D (bottom left)

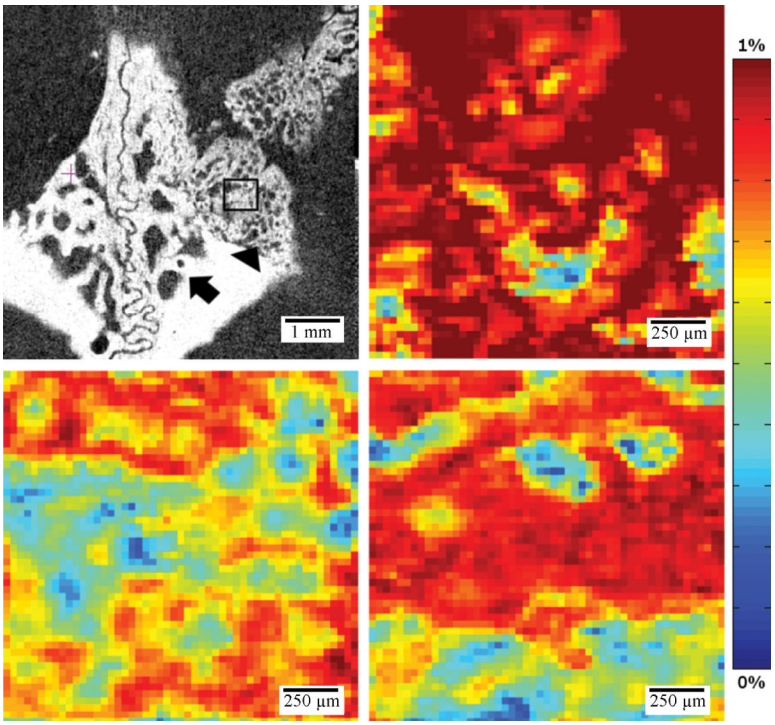

Figure 5.

Representative microCT after reorientation in the cranial/caudal axis (Group D), sample regions of interest (ROI) include native calvarium (arrow), defect margin (arrow head) and defect site (square). Representative model of stress applied to bone trabecula in a sample ROI of native calvarium (top right) and defect site (middle right) and defect margin (bottom right).

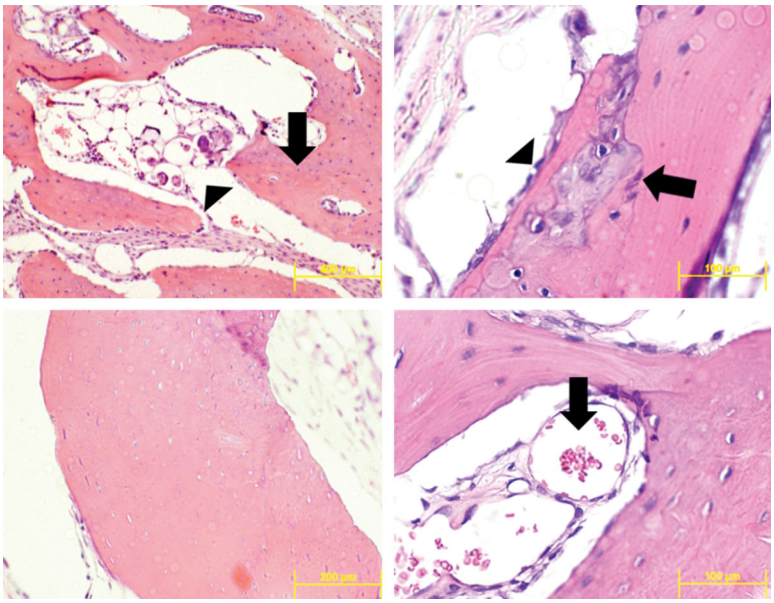

Figure 6.

Representative sections through the center of the defect site with H&E staining. Mature (arrow) found adjacent to the sagittal suture (top left). Newly formed bone (arrow) with microspheres (arrowhead) present within the bone trabeculae (top left). Cartilage intermediate (arrow) within newly formed bone , osteoblasts (arrowhead) line edge of regenerating bone (top right). Neovascularization (arrow) within trabeculae of newly formed bone (bottom right).

Table 1

Experimental Groups

Group	Sample Size (N)	Scaffold	0.1ug rhBMP2	0.1ug PLGA-rhBMP2
A	B			
B	S	X		
C	B	X	X	
D	B	X		X

Table 2

μCT Volume and Surface Area Results

Group	Bone Volume (mm)	Percent Bone Volume (%) (108.51 mm^3)	P Value	Bone Surface Area (mm)	Percent Bone Surface Area (%) (50.24mm^2)	P Value
Empty Defect (A) (N=3)	20.21+/−8.78	18.63+/−8.09	0.025	42.54+/−14.41	84.67+/−28.70	0.025
Scaffold Only (B) (N=5)	30.39+/−15.72	28.01+/−14.49	0.05	45.06+/−14.42	89.70+/−20.06	0.01
0.1ug Free rhBMP2 (C) (N=3)	37.51+/−2.26	34.47+/−2.08	0.025	52.06+/−4.16	103.62+/−8.28	0.025
0.1ug PLGA-rhBMP2 (D) (N=3)	49.25+/−9.13	45.39+/−8.41	-	63.60+/−6.95	126.58+/−13.84	-

Table 3

Regional Tissue Modulus / Apparent Stiffness

Group	Apparent Stiffness (GPa)	P Value
Native Calvarium (N=7)	10.66 +/− 3.07	-
Defect (N=14)	8.31 +/− 2.15	0.07
Control Defect (N=8)	8.64 +/− 2.03	-
Regenerate w/rhBMP2 exposure (N=6)	7.87 +/− 2.42	0.70
Defect Margin (N=14)	10.63 +/− 2.52	-
Native Calvarium (N=7)	10.66 +/− 3.07	0.88
Control (N=8)	8.64 +/− 2.03	0.017
Regenerate w/ rhBMP2 exposure (N=6)	7.87 +/− 2.42	0.12
Regenerate w/ Free rhBMP2 Exposure (N=3)	7.01 +/− 1.07	
Regenerate w/ PLGA-rhBMP2 Exposure (N=3)	8.74 +/− 3.35	0.83